ADVANCED FUNCTIONAL MATERIALS



DOI: 10.1002/adfm.200800017

# Temperature-Induced Size-Control of Bioactive Surface Patterns**

By *Leonid Ionov,** *Alla Synytska,* and *Stefan Diez*

We present a novel method to produce bioactive surface patterns whose size can be changed in response to a variation of the environmental conditions, rather than local treatment. Our approach is based on the structured surface-immobilization of thermoresponsive poly(*N*-isopropylacrylamide) (PNIPAM) polymer chains with different transition temperatures. We experimentally demonstrate how the size of an area in which a particular polymer is collapsed or swollen can be controlled by ambient temperature. We show the temperature-induced size-control of a bioactive surface pattern by embedding functional motor proteins into the switchable polymer layers.

## 1. Introduction

Micropatterned surfaces are widely used for biotechnological applications such as cell culture, bioanalytics, and tissue engineering.[1–8] Although many approaches exist to fabricate sophisticated surface patterns, for example based on microcontact printing, electron beam lithography, or dip-pen lithography[1–5,9–11], they are almost entirely limited to producing fixed patterns that can not be intentionally modified under physiological conditions. However, patterns that could be generated or modified on demand in aqueous environment would tremendously extend the applicability of structured surfaces. In order to achieve such *in-situ* treatment in a localized manner a number of optical[12–15] and electrochemical techniques have been proposed.[16–19] For example, structured illumination of a surface containing light-sensitive groups was used to irreversibly add and remove pattern elements.[14,20] Reconfigurable optical patterning was shown based on reversibly-isomerizable chemical groups[13,15] and application of such surfaces was demonstrated for light-programmed cell adsorption.[12,13] However, most of the optical strategies use UV illumination, which is often harmful to biological species.

Here we demonstrate a new method to produce bioactive surfaces with patterns whose size can be changed in response to variation of the environmental conditions, rather than local treatment. Our design is based on the patterned surface-immobilization of thermoresponsive poly(*N*-isopropylacrylamide) (PNIPAM) polymer chains. In aqueous environments, PNIPAM (homopolymer) chains undergo reversible collapse or swelling above or below the Low Critical Solution Temperature (LCST = 33 °C), respectively. However, the LCST can be gradually increased or decreased by incorporation of additional hydrophobic or hydrophilic comonomers, respectively. Likewise, the LCST can be tuned by varying the ratio of both added comonomer types. Using this principle, we fabricated a surface containing lateral LCST gradients by laying down opposing gradients of hydrophilic and hydrophobic PNIPAM-copolymers (Fig. 1a–c). Across this surface, polymers whose LCST is above or below the actual temperature of the surrounding were collapsed or swollen, respectively. We further showed that changes in ambient temperature could alter the size of the area in which a particular polymer was collapsed or swollen (Fig. 1d). By embedding functional proteins into the switchable polymer layers we demonstrated the temperature-induced size-control of bioactive surface patterns.

## 2. Results and Discussion

First, we prepared and characterized the thermal behavior of the different thermoresponsive PNIPAM copolymers. Random copolymers with hydrophobic *tert*-butyl acrylate (tBA) and hydrophilic acrylic acid (AA) comonomers were synthesized. The hydrophobic tBA monomer units included in the PNIPAM chains (% tBA = 6 mol % in monomer mixture) reduced the LCST to about 25 °C as measured in a pure aqueous environment. The tBA was hydrolyzed into hydrophilic acrylic acid (AA) in an acidic environment (Fig. 2). The LCST of poly(NIPAM-AA) was found to be 33 °C in a pure

[*] Dr. L. Ionov, Dr. S. Diez
Max-Planck-Institute of Molecular Cell Biology and Genetics
Pfotenhauerstrasse 108, 01307 Dresden (Germany)
E-mail: ionov@mpi-cbg.de
Dr. A. Synytska
Leibniz Institute of Polymer Research Dresden e.V.
Hohe Strasse 6, 01069 Dresden (Germany)

[**] The authors are grateful to Prof. Manfred Stamm and the Leibniz Institute of Polymer Research Dresden for the opportunity to perform polymer synthetic experiments. Hartmut Komber (Leibniz Institute of Polymer Research Dresden) is acknowledged for NMR investigations. Wolfgang Birnbaum and Dirk Kuckling (TU Dresden) are acknowledged for the determination of the polymer molecular masses. The kind help of Chris Gell (MPI-CBG) and Laurel Rohde (CRTD Dresden) on the manuscript was highly appreciated. This work was supported by the BMBF (Grant 03N8712), the Volkswagen Foundation and the Max-Planck-Society.

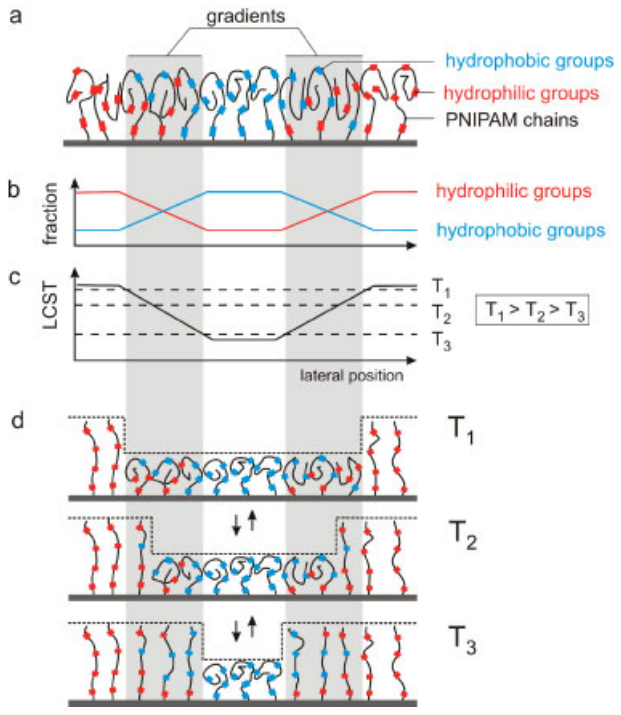


**Figure 1.** Concept of surfaces with size-controlled patterns. a) and b) Lateral gradients of thermoresponsive PNIPAM copolymers with hydrophobic or hydrophilic groups are formed on the surface. c) The Low Critical Solution Temperature (LCST) of PNIPAM copolymers changes gradually with the ratio of hydrophobic to hydrophilic groups. The dashed lines indicate three examples of ambient temperatures $T_1$, $T_2$, and $T_3$. d) Polymer chains with an LCST below and above ambient temperatures $T_1$, $T_2$, and $T_3$ are collapsed and swollen, respectively. As a result, the size of the area containing the collapsed polymer depends on the ambient temperature and can be reversibly tuned.

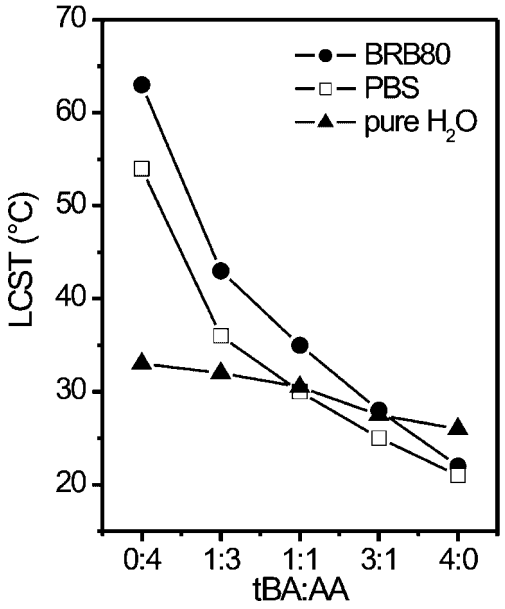


**Figure 3.** The LCST of poly(NIPAM-tBA-AA) copolymers (% tBA + % AA in monomer mixture is 6 mol %) in different aqueous environments: 80 mM Brinkley Reassembly Buffer (BRB80, pH = 6.9), 100 mM Phosphate Bufered Saline (PBS, pH = 7.5) and pure water.

aqueous environment and 50–65 °C in salty buffer solutions (points at tBA:AA = 0:4 ratio in Fig. 3).

To demonstrate that the LCST of poly(NIPAM-tBA-AA) copolymers gradually changes with the ratio of hydrophilic to hydrophobic components, we prepared a series of poly (NIPAM-tBA-AA) copolymers containing different tBA to AA ratios. As expected, the LCST decreased gradually as the tBA to AA ratio increased (Fig. 3). Moreover, the LCST depended on the ionic strength of the aqueous solution. Attributable to changing the balance between intramolecular hydrogen bonds and hydrogen bonds with water[21] an increase in ionic strength lead to (i) a pronounced increase in the LCST of PNIPAM copolymers that have AA as the predominant co-monomer and (ii) a decrease in the LCST for PNIPAM copolymers that have tBA as the predominant co-monomer.

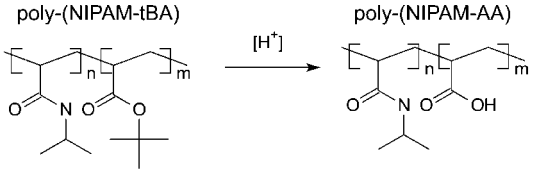


**Figure 2.** Hydrolysis of poly(NIPAM-tBA) copolymer to poly(NIPAM-AA) in an acidic environment.

Next, we fabricated surface-immobilized PNIPAM copolymer layers and investigated their swelling behavior. A poly(NIPAM-tBA) layer grafted to the surface of the silicon wafer was prepared using surface-initiated atom-transfer radical polymerization (see Experimental).[22] The thickness of the polymer layer in the dry state was $h_{DRY} = 33$ nm, and the polymer molecular weight was $M_w = 253000$, polymer dispersity index PDI = 1.8. A poly(NIPAM-AA) layer was obtained by hydrolysis of the poly(NIPAM-tBA) layer in methanesulfonic acid.[23] Ellipsometric investigations revealed that the poly(NIPAM-AA) layer was thicker than the poly(NIPAM-tBA) layer at both high and low temperatures as the result of electrostatic repulsions between negatively charged carboxylic groups (Table 1).

To visually inspect the swelling of both poly(NIPAM-tBA) and poly(NIPAM-AA) layers in a spatially resolved manner, we adsorbed fluorescent protein onto the polymer layers and employed fluorescence interference contrast (FLIC) microscopy.[24] FLIC microscopy is based on interference effects between the direct excitation and emission light with reflected light from the surface leading to a periodic modulation of the detected emission intensity as function of height above the surface (Fig. 4a). Due to a half wavelength phase shift upon reflection on the mirror (silica-silicon interface), fluorescent molecules are almost invisible if located directly on the mirror. The intensity increases as the distance between the fluorescent molecules and the mirror grows, and it passes through the maximum at a distance of about a quarter of a wavelength.

ADVANCED FUNCTIONAL MATERIALS



**Table 1.** Height h and refractive index n of poly(NIPAM-tBA) and poly (NIPAM-AA) grafted layers obtained by ellipsometry in BRB80 at different temperatures. The initial thickness of the poly(NIPAM-tBA) layer in dry state was $h_{DRY} = 33$ nm.

| Polymer | $T$ [°C] | $h$ [nm] | $n$ | $h \times n$ [nm] |
|---|---|---|---|---|
| poly(NIPAM-tBA) | 16 | 86.2 | 1.39 | 120 |
| | 55 | 27.2 | 1.52 | 42 |
| poly(NIPAM-AA) | 16 | 118.7 | 1.37 | 163 |
| | 55 | 46.9 | 1.44 | 67 |

FLIC microscopy thus allows obtaining information about the vertical position of fluorescent objects in the vicinity to a reflecting surface with high spatial accuracy.[25,26]. The intensity can be expressed by the following equation:[27]

$$I(h) = I_0\left(2\cdot(1-r_f)^2 + 8r_f\sin^2\left(\frac{2\pi}{\lambda_{EX}}(n_{SiO2}\cdot h_{SiO2} + n_{PGMA}\cdot h_{PGMA} + n_{PNIPAM}\cdot h)\right)\right) \times \left(2\cdot(1-r_f)^2 + 8r_f\sin^2\left(\frac{2\pi}{\lambda_{EM}}(n_{SiO2}\cdot h_{SiO2} + n_{PGMA}\cdot h_{PGMA} + n_{PNIPAM}\cdot h)\right)\right) \quad (1)$$

where, $I_0$ serves as a proportionality factor. Refractive indices for the PNIPAM layer, PGMA with initiator and $SiO_2$ are represented by $n_{PNIPAM}$, $n_{PGMA} = 1.5$ and $n_{SiO2} = 1.46$. $h_{SiO2} = 1.4$ nm is the oxide thickness, $h_{PGMA} = 2.2$ nm is the height of PGMA layer, and $h$ is the height of the fluorophores above the oxide surface. The reflection coefficient is represented by $r_f$. A set of optical filters defining the excitation and emission wavelengths, $\lambda_{EX} = 565$ nm and $\lambda_{EM} = 610$ nm, has been used.

Experimentally, we incubated the polymer layers with rhodamine-labelled tubulin (1 mg ml$^{-1}$ in BRB80 buffer) at $T = 65$ °C. Because, both the poly(NIPAM-tBA) and poly(-NIPAM-AA) layers were collapsed at this temperature, the tubulin molecules readily adsorbed onto the polymer surface.[28] Unabsorbed protein was removed by multiple rinsing in BRB80 buffer at 18 °C where the polymer chains were swollen. When imaging the surfaces by FLIC microscopy at low temperature ($T < 20$ °C, when both polymers were swollen) we found that the poly(NIPAM-tBA) area was brighter than the poly(NIPAM-AA) area (Fig. 4b). The opposite behavior was observed when the polymers were collapsed high temperature ($T = 55$ °C). We note that this change in fluorescence intensity mainly originated from the changed distance of the fluorescent proteins from the surface rather than from desorption or temperature induced changes in the quantum yield of the fluorophores.[29] To clarify the differences in the fluorescence intensities of poly(NIPAM-tBA) and poly(NIPAM-AA) areas we refer to the polymer layer thicknesses and refractive index values as measured by ellipsometry (Table 1). Considering the ellipsometric results, we expected that the intensity of the collapsed poly(NIPAM-AA) and collapsed poly(NIPAM-tBA) areas must be relatively low because the $h \times n$ values correspond to a position close to the first minimum on the FLIC curve (Table 1, Fig. 4c). The $h \times n$ values of the swollen poly(NIPAM-tBA) and swollen poly(NIPAM-AA) areas correspond to the positions right before and after the first maximum, respectively, and the apparent fluorescence is predicted to be strong. Thus the observed degree of fluorescence in poly(NIPAM-tBA) area is consistent with our expectation (Fig. 4c and d). The difference between the expected and observed behavior in the collapsed and swollen states of the poly(NIPAM-AA) area was likely caused by a larger thickness of the poly(NIPAM-AA) layer than detected by ellipsometry.

To directly investigate the switching of the polymer layers by FLIC microscopy we prepared a flow channel (3 mm × 18 mm × 0.1 mm) between a glass coverslip and the silicon

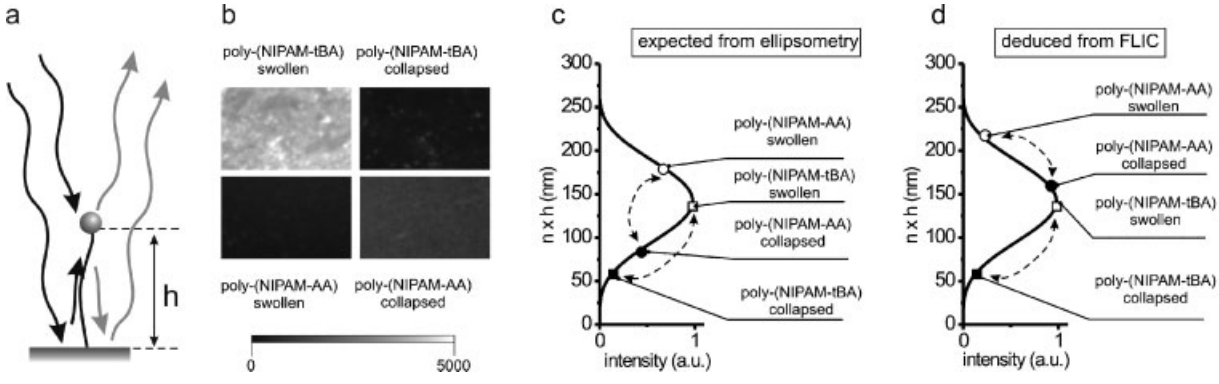


**Figure 4.** Fluorescent Interference Contrast (FLIC) microscopy of poly(NIPAM-tBA) and poly(NIPAM-AA) surfaces. a) Interference of exciting (black line) and emitted (gray line) light near a reflecting surface. b) Observed fluorescence of rhodamine-labelled tubulin adsorbed onto poly(NIPAM-tBA) and poly(NIPAM-tBA) layers in swollen ($T < 20$ °C) and collapsed ($T = 55$ °C) states. c) and d) $h \times n$ values for poly(NIPAM-tBA) (squares) and poly (NIPAM-AA) (circles) layers in swollen (open symbols) and collapsed (solid symbols) states as measured by ellipsometry (measured height values are projected onto the theoretical FLIC curve (c) and deduced from FLIC (measured intensity values are projected onto the theoretical FLIC curve (d).

  

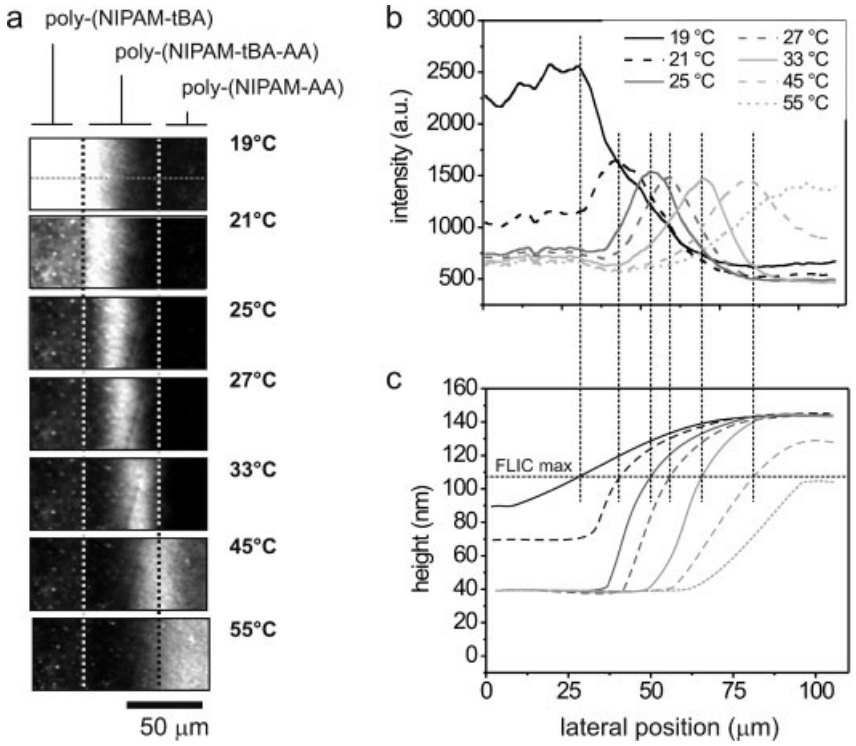


**Figure 5.** Switching of the height profile of the poly(NIPAM-tBA-AA) gradient layer. a) FLIC images of the poly(NIPAM-tBA-AA) layer with adsorbed rhodamine-labeled tubulin at different temperatures. Intensity profile (b) and qualitatively reconstructed height profile (c) along gray dotted line in (a) of the polymer layer at different temperatures. The initial thickness of the poly(NIPAM-tBA) layer in the dry state was $h_{DRY} = 33$ nm.

chip with the polymer layer using double-stick tape. The channel was filled half with water and half with methanesulfonic acid. Due to diffusion at the boundary between water and methanesulfonic acid a gradient of poly(NIPAM-tBA-AA) was formed amidst the fully hydrolyzed poly(NIPAM-AA) and the unhydrolyzed poly(NIPAM-tBA) areas. After about 20 s the channel was rinsed with water from the opposite side. FLIC images of adsorbed fluorescent tubulin (same preparation as described above) revealed a strong fluorescent signal on the poly(NIPAM-tBA) area and a weak signal at the poly(NIPAM-AA) area at low temperature ($T < 20\,^{\circ}C$) (Fig. 5a). At high temperature ($T > 50^{\circ}C$) the poly(NIPAM-AA) appeared brighter than the poly(NIPAM-tBA) area. This behavior was expected from the results shown in Figure 4. However, most interestingly, a bright, spatially confined band in the poly(NIPAM-tBA-AA) gradient area was detected at temperatures between 21 °C and 50 °C.

Considering equation 1, this bright band represents the maximum of the FLIC curve at $n \times h \approx 140$ nm (see also Fig. 4c and d). The lateral coordinate of this band shifted towards the poly(NIPAM-AA) areas when the temperature increased (Fig. 5b). This directly indicates that the height and/or refractive index profile of the polymer layer changes with temperature. Since the difference in the refractive indicies in the swollen versus the collapsed polymers is rather small – namely $100\% \times n_{collapsed} - n_{swollen}/n_{collapsed} = 100\% \times (1.52 - 1.37)/1.52 \approx 10\%$ (Table 1) – the change in the intensity profile along the sample was mainly caused by changes in the height of the polymer layer. A qualitative reconstruction of the height profile of the polymer layer at different temperatures is shown in Figure 5c.[30] Here, one can see an obvious gradual shift of the border between the swollen and the collapsed areas. This border was not completely step-like due to the unsharp transition between the collapsed and the swollen polymer chain conformations. In this particular experiment, the border between the collapsed and the swollen areas was reversibly shifted by about 50 μm, but shifts up to 120 μm were obtained in additional experiments. Importantly, the changes in the size of the collapsed and the swollen areas were fully reversible (data not shown).

In order to fabricate circular patterns whose diameter can be controlled by temperature, we synthesized a thermoresponsive polymer layer based on random copolymerization of NIPAM with hydrophobic photoliable 2-nitrobenzyl acrylate (NBA). The LCST of the poly(NIPAM-NBA) copolymer ($M_w = 114000$, PDI = 1.7, obtained by polymerization of a mixture of

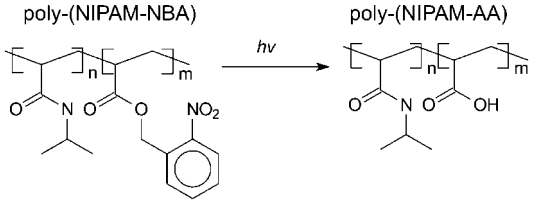


**Figure 6.** Conversion of poly(NIPAM-NBA) copolymer into poly(NIPAM-AA) upon UV illumination.

ADVANCED FUNCTIONAL MATERIALS



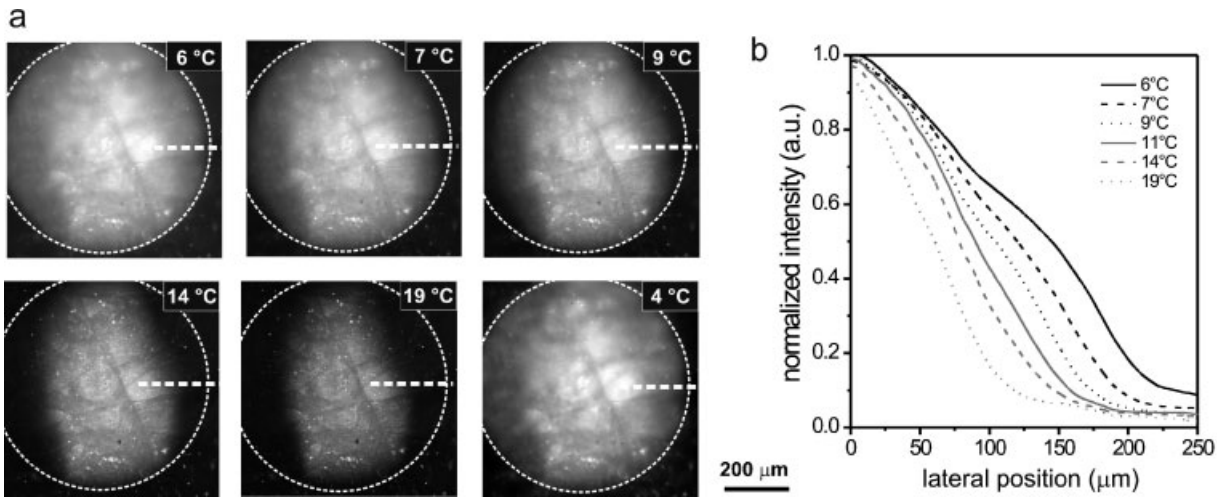


**Figure 7.** Switching the size of a circular poly(NIPAM-NBA-AA) pattern. a) FLIC images of rhodamine-labelled tubulin on poly(NIPAM-NBA-AA) pattern at different temperatures. The size of the swollen (bright) area changes with temperature. b) Normalized fluorescence intensity profiles of the polymer layer at different temperatures along the white dashed line in (a). The initial thickness of the poly(NIPAM-NBA) layer in the dry state was $h_{DRY} = 15.7$ nm

94 mol % NIPAM and 6 mol % NBA) was about 7 °C in BRB80 buffer. We then illuminated a part of the poly(NIPAM-NBA) layer with UV light ($\lambda = 360$ nm) using a 100× microscope objective. This resulted in the localized cleavage (deprotection) of the hydrophobic 2-nitrobenzyl groups and the formation of hydrophilic carboxylic groups (Fig. 6) in a circular area with diameter of about 0.5 mm. The LCST of the fully deprotected polymer was more than 90 °C. Because, in our case, the degree of deprotection gradually decreased from the center of the illuminated area towards the edges we obtained a two-dimensional poly(NIPAM-NBA-AA) gradient.

Using FLIC microscopy (with fluorescent tubulin, as described above) we observed a decrease in the fluorescence intensity in the center of the deprotected area as well as a decrease in the size of the bright area upon raising the temperature (Fig. 7a and b). This behavior is attributed to the collapse of the polymer chains and thus a decrease in the detected fluorescence intensity in a spatially varying manner. Remarkably, when the temperature was lowered back to the initial value the size of the swollen area was fully recovered (Fig. 7a, lower right image). This observation indicates the reversibility of the switching process. We note, that smaller patterns can be fabricated on demand by UV-illumination through a mask.[31]

To demonstrate the temperature-induced size-control of bioactive surface patterns, we assayed the gliding motility of microtubules on kinesin-coated poly(NIPAM-tBA-AA) gradient surfaces. Microtubules are hollow, cylindrical, protein filaments with an outer diameter of 24 nm. They can be formed *in vitro* by self-assembly of tubulin-heterodimers reaching lengths of up to several tens of micrometers. Kinesin[32,33] is an ATP-hydrolysing enzyme that moves vesicles and organelles along microtubules in a cellular environment.[34] Recently, it was shown that microtubules can reversibly land and release (in response to collapsing and swelling of the polymer chains) on composite surfaces where kinesin molecules were embedded in a homopolymer PNIPAM layer.[35] Here, we adsorbed kinesin on poly(NIPAM-tBA-AA) gradient surfaces (similar to those presented in Fig. 5a) at $T = 37$ °C. We then lowered the temperature to 17 °C which caused swelling of both poly(NIPAM-tBA) and poly(NIPAM-AA) and led to the release of weakly adsorbed kinesin. We then imaged the gliding motility of rhodamine-labelled microtubules on the kinesin molecules that were entrapped in the thin polymer layer by timelapse fluorescence microscopy. At a temperature of $T = 21$ °C, which is slightly above the LCST of poly(NIPAM-tBA), we found that microtubules were gliding only on the poly(NIPAM-tBA) surface area where the polymer chains were collapsed and did not repel the microtubules (Fig. 8). Increasing the temperature up to $T = 41$ °C led to a laterally progressing collapse of the poly(NIPAM-tBA-AA) and allowed the microtubules to land on the exposed kinesin molecules in the gradient area. Cooling back down to $T = 21$ °C deactivated the poly(NIPAM-tBA-AA) gradient area again. The associated swelling of the polymer chains repelled the gliding microtubules and prevented the landing of microtubules on the kinesin molecules in this area. This reversible size control of the active kinesin pattern could be repeated multiple times.

## 3. Conclusions

In summary, we presented a new concept to design bioactive patterned surfaces whose size can be controlled by altering the ambient conditions. In one set of experiment, we generated

  

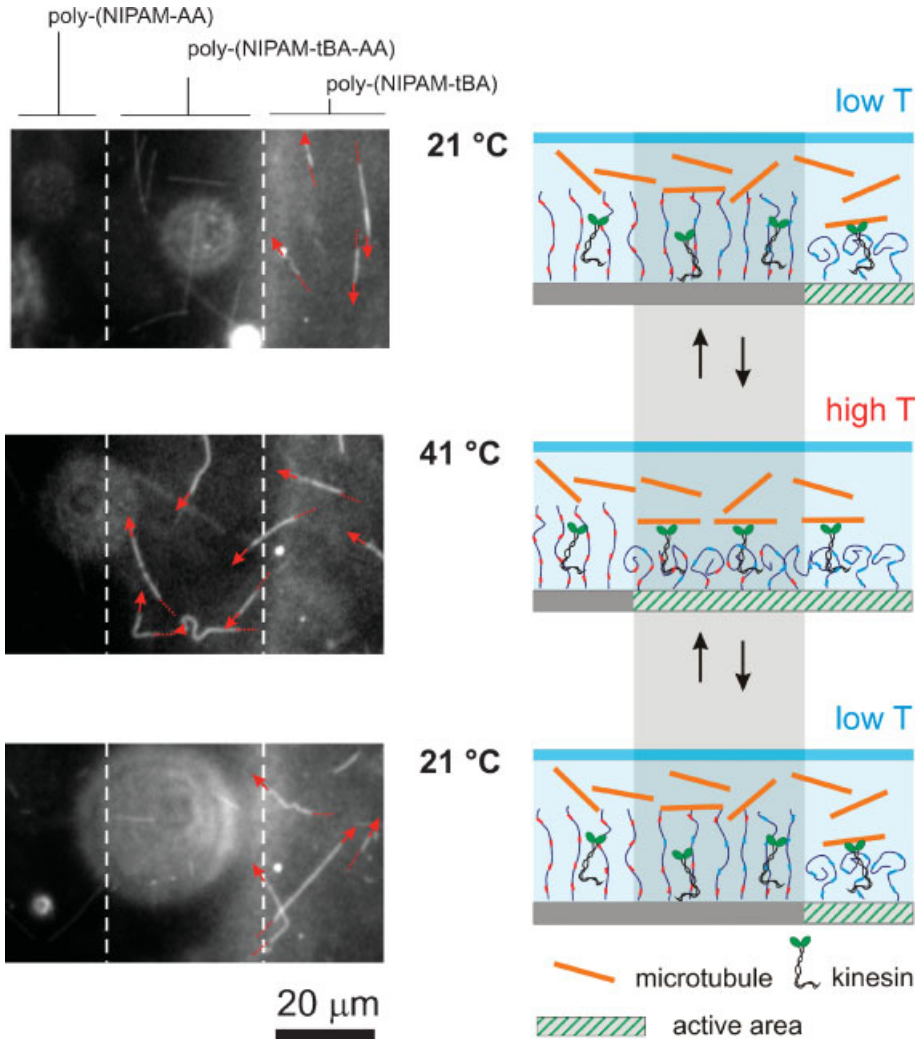


**Figure 8.** Temperature-induced size-control of bioactive surface patterns. Left panel: Fluorescence images of rhodamine-labeled microtubules driven by kinesin motors on a substrate surface with grafted poly(NIPAM-tBA-AA) gradient. Actively gliding microtubules were determined by timelapse microscopy and are indicated by the red arrowheads (direction of movement) and the dotted lines (traveled path during the preceding frames). White circular patterns in the fluorescent images arise from microtubules, which are diffusing in solution out of focus. Right panel: Schematic diagram of polymer conformation and gliding motility. Repeated changes in temperature resulted in the reversible switching of the polymer chains between the extended conformation (repelling microtubules from the surface) and the collapsed conformation (enabling gliding motility of microtubules).

lateral gradients composed of thermoresponsive poly(*N*-isopropylacryl amide – *tert*-butyl acrylate – acrylic acid) copolymers by local hydrolysis using methanesulfonic acid. On these gradients we showed that the border between the collapsed and the swollen polymer areas could be reversibly shifted by up to 120 μm when raising or lowering the temperature between 21 °C and 50 °C. Utilizing kinesin-driven motility of microtubules, we demonstrated the applicability of these gradients for the temperature-induced size-control of bioactive surface patterns. In a second set of experiments we generated circular gradients of poly(*N*-isopropylacryl amide – 2-nitrobenzyl acrylate – acrylic acid) by UV irradiation. It is thus possible to use photolithography to produce switchable polymer gradients with customized layouts. We note, that the temperature range over which switching occurs can be precisely tuned by selecting the appropriate copolymer composition. We believe that this novel strategy to produce surface patterns whose size and shape can be reversibly switched *in-situ* will be of interest for a variety of biotechnological applications, such as programmed cell adhesion, viability and differentiation.

## 4. Experimental

*Materials*: Highly polished single-crystal silicon wafers of {100} orientation (Semiconductor Processing Co.) were used as a substrate. *N*-isopropylacrylamide (NIPAM, Aldrich), acetone (Aldrich), *N*,*N*,*N*′,

ADVANCED FUNCTIONAL MATERIALS



*N*″,*N*″-pentamethyldiethylenetriamine (PMDTA, Aldrich), ethyl-2-bromoisobutyrate (EBiB), ethylenediamine (ED, Fluka), anhydrous dichloromethane (Aldrich), 2-bromo-2-methylpropanoyl bromide (BMPB, Aldrich) triethylamine (Fluka), L-ascorbic acid (Sigma), copper bromide (Aldrich), 2,2′-azobis(2-methylpropionitrile) (AIBN), methane sulfonic acid (Merck) were used as received. *tert*-butyl acrylate (tBA, Fluka) was distilled under nitrogen steam prior to polymerization. Polyglycidyl methacrylate (PGMA) ($M_n = 84\,000\,g\,mol^{-1}$) was synthesized by free radical polymerization of glycidyl methacrylate (Aldrich).

*Synthesis of 2-Nitrobenzyl Acrylate (NBA)*: 3 g ($1.9 \times 10^{-2}$ mol) of 2-nitrobenzyl alcohol, 2.1 g ($2 \times 10^{-2}$ mol) of triethylamine were dissolved in 20 ml of anhydrous dichloromethane, and 1.7 ml ($2 \times 10^{-2}$ mole) of acryloyl chloride was added drop-wise to the resulting solution. Stirring continued for one hour. After filtering out the resulting salt, the filtrate was concentrated and purified by column chromatography (packed material: silica gel; eluent: hexane/ethyl acetate = 10/1). Thus, 2.7 g of an oily liquid was recovered and confirmed to be 2-nitrobenzyl acrylate by NMR spectroscopy. $^1$H-NMR (500.13MHz, $CDCl_3$ $\delta$): 5.6 (s, 2H), 5.8–6.5 (m, 3H), 7.1–8.1 (m, 4H).

*Synthesis of Poly(NIPAM-tBA-AA) Random Copolymers*: Poly (NIPAM-tBA-AA) random copolymers were synthesized by free radical polymerization. For this, 2 g (0.0177 mol) of NIPAM, *tert*-butyl acrylate and acrylic acid (total $1.12 \times 10^{-3}$ mol) and 8 mg of AIBN ($4.9 \times 10^{-5}$ mol) were dissolved in 4 ml acetone. Polymerization was carried out in an argon atmosphere for 1.5 h.

*Surface-Initiated Polymerization*: The silicon wafers were first cleaned in an ultrasonic bath for 30 min, placed in a hot piranha solution (3:1 concentrated sulphuric acid and 30% hydrogen peroxide; the mixture reacts violently with organic solvents and should be handled with care) for 1 h, and then rinsed several times with MilliQ water. The thickness of silicon oxide was measured to be 1.3 nm after the cleaning procedure. A thin layer of PGMA (1.75 nm) was deposited on top of the chips by spincoating 0.02% PGMA solution in chloroform at 2000 rpm and annealing at 110 °C for 10 min. Afterwards, the wafers were rinsed in a 1.5% ethanol solution of ethylenediamine (ED) for 2 h. The wafers were carefully rinsed in 2× in ethanol, 2× in ethanol/water mixture in ultrasonic bath and dried with nitrogen flux. The thickness of the PGMA + ED layer was 1.65 nm. The wafers were rinsed in a solution of BMPB (0.96 g, $4.2 \times 10^{-3}$ mol) and triethylamine (0.72 g, $7 \times 10^{-3}$ mol) in anhydrous dichloromethane (100 ml). The wafer were rinsed in dichloromethane 2× and dried with nitrogen flux. The thickness of the PGMA + ED + BMPB layer was 1.85 nm.

Poly(NIPAM-tBA) and poly(NIPAM-NBA) random copolymer brushes were prepared as follows: NIPAM (4 g, $3.5 \times 10^{-2}$ mol), tBA (288 mg, $2.25 \times 10^{-3}$ mol) or NBA (465 mg, $2.25 \times 10^{-3}$ mol) EBIB (8 mg, $4.1 \times 10^{-5}$ mol) were dissolved in 6 ml of acetone solution of $CuBr_2$ (0.4 mg, $1.8 \times 10^{-6}$ mol) and PMDTA (0.31 mg, $1.8 \times 10^{-6}$ mol). The reaction solution was added to the tube containing the wafer with immobilized initiator. After the tube was sealed with a rubber septum, a solution of L-ascorbic acid (18 mg, $1 \times 10^{-4}$ mol) in water (0.5 ml) was injected. The vial was placed in a 70 °C oil bath. The polymerization was carried out under stirring and was stopped after 4 h.

*Ellipsometry*: The thickness of the polymer layers was measured at $\lambda = 633$ nm and an angle of incidence of 70° with a SENTECH SE-402 microfocus ellipsometer as described elsewhere [36,37].

*Fluorescent Microscopy*: Fluorescence images were obtained using an Axiovert 200M inverted microscope with a 20× objective (Zeiss, Oberkochen, Germany) equipped with FluoArc lamp. For data acquisition a standard TRITC filterset (excitation: HQ 535/50; dichroic: Q 565 LP; emission: HQ 610/75, Chroma Technology) in conjunction with a Micromax 512 BFT camera (Photometrics, Tucson, AZ) and a MetaMorph imaging system (Universal Imaging, Downingtown, PA) were used.

Received: January 01, 2008


[1] A. Khademhosseini, R. Langer, J. Borenstein, J. P. Vacanti, *Proc. Natl. Acad. Sci. USA* **2006**, *103*, 2480.
[2] A. Folch, M. Toner, *Annu. Rev. Biomed. Eng.* **2000**, *2*, 227.
[3] N. Li, A. Tourovskaia, A. Folch, *Crit. Rev. Biomed. Eng.* **2003**, *31*, 423.
[4] S. Raghavan, C. S. Chen, *Adv. Mater.* **2004**, *16*, 1303.
[5] N. Sniadecki, R. A. Desai, S. A. Ruiz, C. S. Chen, *Ann. Biomed. Eng.* **2006**, *34*, 59.
[6] D. Falconnet, G. Csucs, H. M. Grandin, M. Textor, *Biomaterials* **2006**, *27*, 3044.
[7] C. S. Chen, M. Mrksich, S. Huang, G. M. Whitesides, D. E. Ingber, *Science* **1997**, *276*, 1425.
[8] R. McBeath, D. M. Pirone, C. M. Nelson, K. Bhadriraju, C. S. Chen, *Develop. Cell* **2004**, *6*, 483.
[9] Y. N. Xia, G. M. Whitesides, *Angew. Chem. Int. Ed.* **1998**, *37*, 551.
[10] R. D. Piner, J. Zhu, F. Xu, S. H. Hong, C. A. Mirkin, *Science* **1999**, *283*, 661.
[11] Y. N. Xia, J. A. Rogers, K. E. Paul, G. M. Whitesides, *Chem. Rev.* **1999**, *99*, 1823.
[12] J. Edahiro, K. Sumaru, Y. Tada, K. Ohi, T. Takagi, M. Kameda, T. Shinbo, T. Kanamori, Y. Yoshimi, *Biomacromolecules* **2005**, *6*, 970.
[13] A. Higuchi, A. Hamamura, Y. Shindo, H. Kitamura, B. O. Yoon, T. Mori, T. Uyama, A. Umezawa, *Biomacromolecules* **2004**, *5*, 1770.
[14] J. Nakanishi, Y. Kikuchi, T. Takarada, H. Nakayama, K. Yamaguchi, M. Maeda, *J. Am. Chem. Soc.* **2004**, *126*, 16314.
[15] H. S. Lim, J. T. Han, D. Kwak, M. H. Jin, K. Cho, *J. Am. Chem. Soc.* **2006**, *128*, 14458.
[16] C. Zhao, I. Witte, G. Wittstock, *Angew. Chem. Int. Ed.* **2006**, *45*, 5469.
[17] H. Kaji, M. Kanada, D. Oyamatsu, T. Matsue, M. Nishizawa, *Langmuir* **2004**, *20*, 16.
[18] H. Kaji, K. Tsukidate, T. Matsue, M. Nishizawa, *J. Am. Chem. Soc.* **2004**, *126*, 15026.
[19] X. Y. Jiang, R. Ferrigno, M. Mrksich, G. M. Whitesides, *J. Am. Chem. Soc.* **2003**, *125*, 2366.
[20] B. Zhao, J. S. Moore, D. J. Beebe, *Science* **2001**, *291*, 1023.
[21] J. D. Debord, L. A. Lyon, *Langmuir* **2003**, *19*, 7662.
[22] K. Matyjaszewski, H. C. Dong, W. Jakubowski, J. Pietrasik, A. Kusumo, *Langmuir* **2007**, *23*, 4528.
[23] A. Synytska, M. Stamm, S. Diez, L. Ionov, *Langmuir* **2007**, *23*, 5205.
[24] A. Lambacher, P. Fromherz, *Appl. Phys. A* **1996**, *63*, 207.
[25] J. Kerssemakers, J. Howard, H. Hess, S. Diez, *Proc. Natl. Acad. Sci. USA* **2006**, *103*, 15812.
[26] L. Ionov, S. Sapra, A. Synytska, A. L. Rogach, M. Stamm, S. Diez, *Adv. Mater.* **2006**, *18*, 1453.
[27] Y. Kaizuka, J. T. Groves, *Biophys. J.* **2004**, *86*, 905.
[28] D. L. Huber, R. P. Manginell, M. A. Samara, B.-I. Kim, B. C. Bunker, *Science* **2003**, *301*, 352.
[29] To prove this, we observed the fluorescence of protein adsorbed onto PNIPAM layer grafted onto special silicon chip with set of four different thicknesses of silicon oxide. This experiment, which allows reconstruction of FLIC curve and obtaining the value of $h \times n$ does show that the distance between fluorescent protein and surface change when polymer collapses or swells.
[30] The height profile has been reconstructed taking into account the following consideration. For simplicity, we assumed that refractive index of polymer layer has an intermediate value between that of the polymer in the collapsed and the swollen states ($n = 1.4$). The Maximum of the intensity corresponds to the condition of $n \times h \approx 140$ nm (Fig. 3). The height of the poly(NIPAM-tBA) area corresponds to the position before first maximum and is $h \approx 110$ nm. The intensity profiles have been corrected with respect to changes of intensity of the fluorescence with temperature.


  

[31] J. Opitz, F. Braun, R. Seidel, W. Pompe, B. Voit, M. Mertig, *Nanotechnology* **2004**, *15*, 717.
[32] J. Howard, *Nature* **1997**, *389*, 561.
[33] J. Howard, *Mechanics of Motor Proteins and the Cytoskeleton*, Sinauer Press, Sunderland, MA **2001**.
[34] R. D. Vale, *Cell* **2003**, *112*, 467.
[35] L. Ionov, M. Stamm, S. Diez, *Nano Lett.* **2006**, *6*, **1982**.
[36] S. Minko, S. Patil, V. Datsyuk, F. Simon, K. J. Eichhorn, M. Motornov, D. Usov, I. Tokarev, M. Stamm, *Langmuir* **2002**, *18*, 289.
[37] L. Ionov, A. Sidorenko, K.-J. Eichhorn, M. Stamm, S. Minko, K. Hinrichs, *Langmuir* **2005**, *21*, 8711.